Biological Permanent Magnets

RICHARD B. FRANKEL
Department of Physics, California Polytechnic State University, San Luis Obispo, CA 93407, USA

On the occasion of the 80th birthday of Hendrik de Waard

Abstract. Magnetotactic bacteria orient and migrate along magnetic field lines. Each cell is essentially a self-propelled magnetic dipole. The magnetic properties of these bacteria have been determined by a variety of techniques, including pulsed hysteresis measurements on single cells.

Key words: aerotaxis, electron holography, greigite, magnetite, magnetosomes, magnetotaxis.

1. Introduction

Hendrik de Waard is best known for his contributions to electronics, radio communications, condensed matter physics, nuclear physics and Mössbauer spectroscopy. His contributions to biophysics are less known because they came late in his career. In 1993, Hendrik came to Cal Poly-San Luis Obispo as a visiting professor and became fascinated by magnetotactic bacteria. We initiated a research program that was pursued during subsequent visits and resulted in two publications [1, 2]. In this paper I will briefly review the current situation regarding the magnetic properties of these bacteria in honor of Hendrik's contributions to the field.

2. Magnetotactic bacteria

The ability of motile, aquatic bacteria to orient and migrate along magnetic field lines is known as magnetotaxis [3]. Magnetotactic bacteria comprise a number of species or strains that are indigenous in chemically-stratified water columns or sediments where they occur predominantly at the microaerobic and the anoxic regions of the habitat or both [4]. They are motile by means of flagella; the arrangement of flagella varies between species/strains.

Killed cells orient but do not migrate along magnetic field lines, indicating that each cell has a permanent magnetic dipole that is oriented by the torque exerted by the local magnetic field. Cellular motility results in migration along the magnetic field lines [5]. Thus magnetotactic bacteria are essentially self-propelled magnetic dipoles.

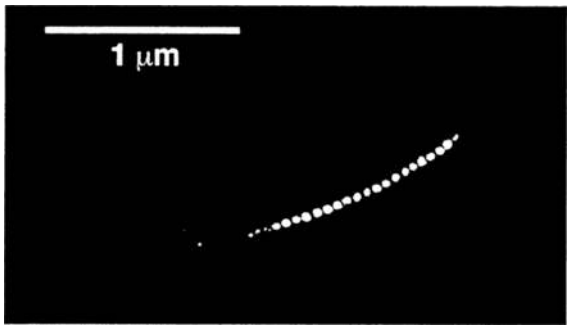

Figure 1. Transmission electron micrograph of *Magnetospirillum magnetotacticum* showing the chain of magnetosomes inside the cell. The magnetite crystals incorporated in the magnetosomes have cuboctahedral morphology and are ca. 42 nm long.

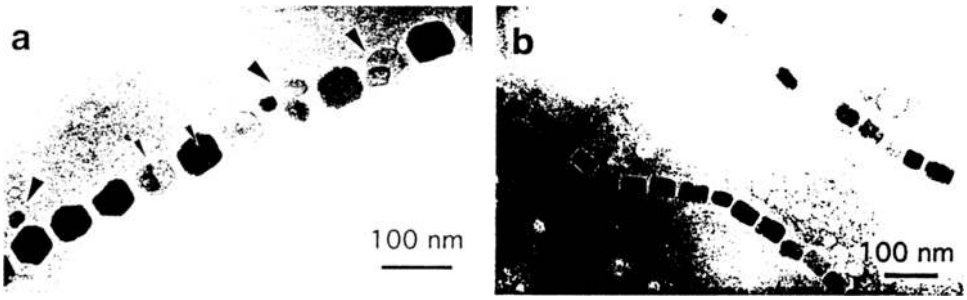

Figure 2. Electron micrographs of magnetosome magnetite crystals in two cultured magnetotactic bacteria. (a) Cuboctahedral crystals in *Magnetospirillum magnetotacticum* (see Figure 1). Small arrows indicate twinned crystals and large arrows indicate clusters of small crystals. (b) Elongated crystals in a marine magnetotactic bacterium, strain MV-1. There are two cells, each with one chain of magnetosomes.

All magnetotactic bacteria contain magnetosomes [6], intracellular structures that are responsible for the cellular magnetic dipole. The magnetosomes comprise magnetite (Fe_3O_4) or greigite (Fe_3S_4) crystals contained in phospholipid membrane vesicles [7, 8]. The magnetosome membrane is presumably a structural entity that is the locus of biological control over the nucleation and growth of the mineral crystal. Almost every magnetotactic species or strain exclusively produces either magnetite or greigite magnetosomes. In the majority of magnetotactic bacteria, the magnetosomes are organized in one or more straight chains of various lengths parallel to the long axis of the cell (Figure 1). There is evidence from Mössbauer spectroscopy of whole cells that the magnetosome chain is fixed within the cell [9], presumably by the magnetosome membrane.

The habits of the magnetosome magnetite crystals appear to be consistent within a given species or strain, although some variation in shape and size can occur within a magnetosome chain. In addition to the roughly isometric crystal shapes, e.g., in magnetosomes in *Magnetospirillum magnetotacticum*, several non-isometric,

elongated shapes occur in other species (Figure 2), including pseudo-prismatic and tooth/bullet shapes [10].

3. Magnetic properties of magnetite magnetosomes

Although variations exist between species, almost all magnetite and greigite magnetosomes fall within a narrow size range of about 35–120 nm when measured along their long axes [11–15]. This size range is significant because it places these grains within the stable magnetic single domain (SD) size range for magnetite and greigite [16]. Grains within the SD size range are uniformly magnetized, which means their magnetic dipole moment is maximum, that is, equal to the saturation moment M_s. Grains larger than about 100 to 120 nm are non-uniformly magnetized because of the formation of multiple magnetic domains, domain walls, or vortex configurations; this has the effect of making their magnetic moments per unit volume significantly smaller than in SD grains. At the other extreme, SD grains smaller than about 30 nm are superparamagnetic (SPM) at ambient temperature, with a remanent magnetization approaching zero. Therefore, magnetotactic bacteria produce the optimum crystal size for maximum moment per unit volume.

4. Magnetic anisotropy of magnetosomes

Magnetite magnetosomes are generally aligned with a [1 1 1] crystallographic axis parallel to the magnetosome chain axis [17]. For elongated crystal habits, the [1 1 1] crystallographic axis aligned along the chain is the elongation axis. In contrast, greigite magnetosomes are aligned with a [1 0 0] crystallographic axis parallel to the chain axis [12]. The significance of the [1 1 1] direction in magnetite is that it corresponds to the magnetic easy axis (defined below). Similarly, the [1 0 0] direction is probably the magnetic easy axis in greigite. No direct determination of easy axis orientation in greigite has yet been made.

The magnetic easy (i.e., low energy) axes arise from anisotropy in the magnetocrystalline energy, resulting from the interaction of spin magnetic moments with the crystalline matrix. In magnetite above 120 K, the [1 1 1] directions are the magnetic easy axes and the [1 0 0] directions are the hard (i.e., high energy) axes [18]. Reversal of the magnetization from one easy axis to another by an applied field requires rotation through a hard axis. The magnetocrystalline anisotropy thus creates an energy barrier that pins M_s along one easy axis until a large enough magnetic field is applied to cause an irreversible jump of M_s over the anisotropy barrier. This magnetic field is related to the coercivity H_c and is a measure of the stability of remanence against remagnetization by time, temperature or magnetic fields. If a grain is elongated, it is shape anisotropy rather than magnetocrystalline anisotropy that inhibits remagnetization during a hysteresis cycle and is another source of coercivity in materials with high saturation magnetization, M_s, such as

magnetite. Shape anisotropy is primarily responsible for the coercivity observed in magnetosomes [19].

5. Magnetosome chains

The arrangement of the single-magnetic-domain magnetosomes in chains maximizes the dipole moment of the cell because magnetic interactions between the magnetosomes cause each magnetosome moment to spontaneously orient parallel to the others along the chain axis. Thus the total dipole moment of the chain, **M**, is the algebraic sum of the moments of the individual magnetosomes in the chain. However, this is true only because the magnetosomes are physically constrained by the magnetosome membranes in the chain configuration. If free to float in the cytoplasm, magnetosomes would likely clump, resulting in a smaller net dipole moment than in the chain. For organisms such as *Magnetospirillum magnetotacticum*, the remanent moment is the maximum possible (saturation) moment of the chain [2, 5].

6. Magnetic properties of magnetosomes at ambient temperatures

A room-temperature hysteresis loop for a bulk magnetotactic bacterial sample exhibits classical SD behavior. The saturation remanence to saturation magnetization ratio, M_r/M_s, is approximately 0.5, which is the theoretical value for a randomly oriented assemblage of SD grains with uniaxial anisotropy [16]. The chain structure effectively removes the equivalence among the different [1 1 1] easy directions and produces a unique easy axis coinciding with the particular [1 1 1] axis aligned along the chain axis.

Hysteresis measurements from a number of different cultured strains of magnetotactic bacteria yield coercivities (H_c) between 20–50 mT, which are larger than the expected theoretical coercivity ($\approx$11 mT) for randomly oriented SD magnetite crystals with magnetocrystalline easy axes along [1 1 1] directions [20]. This indicates that the intrinsic magnetocrystalline anisotropy is not the main source of the coercivity but instead a combination of crystal elongation along [1 1 1] and the linear chain arrangement controls the remagnetization process and pins the magnetization along the chain direction. More significantly, the observed coercivities are much larger than the geomagnetic field (0.05 mT) and demonstrate that changes in the geomagnetic field, even polarity reversals in the geologic past, are not sufficient to remagnetize the polarity of the magnetosome chains. This has been confirmed by magnetic measurements of individual magnetotactic bacteria with single magnetosome chains by Hendrik de Waard and others that show square hysteresis loops with coercive forces of the order of 30 mT [2] and on isolated magnetosomes arranged in chain segments of up to 14 grains [21]. Additional results on room temperature remanence, hysteresis, and demagnetization behavior of whole cells and extracted magnetosomes can be found in [19, 22].

7. Magnetosomes and micromagnetism

While the dimensions of most magnetite magnetosomes place them within the theoretical SD size range, some appear to be much larger than SD and plot within the theoretical multidomain (MD) size range. Examples include large (up to 200 nm) magnetosomes found in coccoid cells from Lagoa de Itaipu, near Rio de Janeiro, Brazil [23, 24].

The existence of the metastable SD (MSD) state provides a possible explanation for the grain dimensions of the anomalously large magnetosomes [19, 25]. As initially uniformly-magnetized magnetosomes nucleate and grow in size from the SPM state to the stable SD state and beyond, it may be energetically favorable for the grains to retain a near uniform SD state (flower state) into the metastable SD range instead of reverting to a non-SD state because the additional activation energy needed for the transformation is not available. Magnetic interactions between magnetosomes along a chain may also help to stabilize the SD structure [25].

According to results from three-dimensional micromagnetic models, the magnetosomes in the coccoid cells from Brazil as well as large magnetosomes in other organisms fall within the predicted MSD range and therefore can quite naturally possess an SD structure. This hypothesis has recently been tested using the technique of off-axis electron holography in a transmission electron microscope. This technique allows the visualization of magnetic structure and correlation with physical structure [26, 27] as discussed below.

8. Magnetosome magnetization from electron holography

In off-axis electron holography in the transmission electron microscope, the sample is positioned so that it covers approximately half the field of view and a charged electrostatic biprism causes the electron wave that has passed through the specimen to overlap with a reference wave that has only passed through vacuum. The resulting hologram is an interference pattern in which amplitude information is contained in the relative amplitude of the cosine-like fringes and information about the phase shift of the electron wave is contained in the fringe positions. The holographic phase data can be decomposed into electrostatic and magnetic contributions and displayed as thickness contours and magnetic field lines, respectively [27].

Superposition of contours of the magnetic contribution to the holographic phase on the electrostatic contribution to the phase allows correlation of the magnetic flux lines with the positions of the magnetosomes. Contours of spacing 0.064 radians are overlaid on the magnetosomes in Figure 3 for a cell of the magnetotactic bacterium *M. magnetotacticum* [26, 27]. The contours provide a semi-quantitative map of the magnetic field in the sample; the direction of the field at each point is tangential to the contour. All the magnetosomes in *M. magnetotacticum* are single magnetic domains magnetized parallel to the axis of the magnetosome chain, in confirmation of the discussion above. For a magnetosome at the end of the chain, the contours "fan out" suggesting a flower state configuration as predicted by

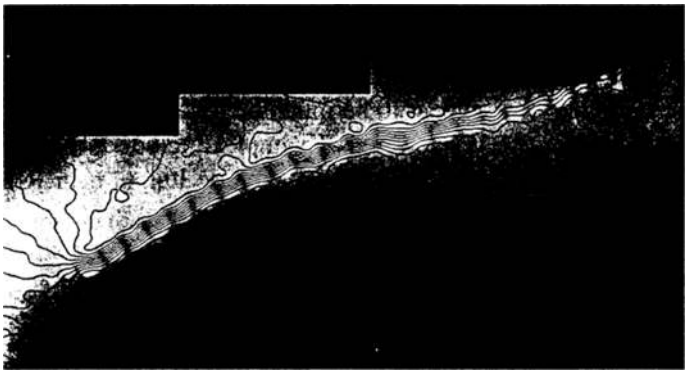

Figure 3. Contours derived from the magnetic contribution to the electron holographic phase overlaid onto positions of the magnetosomes in the cell of *Magnetospirillum magnetotacticum* shown in Figure 1. The contours provide a map of the local magnetic field in the cell. The confinement of the magnetic flux within the magnetosomes shows that all the magnetite crystals are single magnetic domains magnetized approximately parallel to the axis of the chain.

micromagnetic models. At one point in the chain two small magnetosomes have mineralized in place of a larger one, resulting in a slightly poorer, but detectable, confinement of the magnetic field at that point. Smaller crystals at the right end of the chain are in the SPM size range, yet they are also magnetized parallel to the chain axis, presumably by interactions with the magnetic field of the larger crystals in the chain. Finally, the magnetic dipole moment of the magnetosome chain can be obtained from the magnetic contribution to the phase, giving 5×10^{-16} A m^2 (5×10^{-13} emu). This value is consistent with the value predicted for a chain of twenty-two 45 nm diameter spheres of magnetite, using the bulk magnetization 480 kA/m.

Similar measurements have been made with the 200 nm magnetosomes in the bacteria from Brazil [28]. Although a significant amount of magnetic flux could be seen emerging from the sides of the larger magnetosomes, the concentration of flux lines within the crystals showed that the magnetosomes are SD in the chain configuration.

On the other hand, magnetic field patterns in magnetosomes not in chains suggested that these crystals contain domain walls and therefore are not SD in non-chain configurations. Thus it appears that the large magnetosomes are SD only in the chain configuration where they are magnetized by the neighboring crystals [28]. The curvature of the field lines emerging from the sides of the large crystals in the chain is typical of the "flower-like" state predicted by micromagnetic models.

9. Magnetosomes and magnetotaxis

Magnetotaxis results from the passive orientation of magnetotactic bacteria along the local vertical direction of the geomagnetic field by the torque exerted by the field (**B**) on the cellular magnetic dipole moment (**M**) [5]. The thermally averaged

projection of the dipole moment on the magnetic field is given by the Langevin function

$$\langle \cos\theta \rangle = L(\alpha) = \coth(\alpha) - 1/\alpha,$$

where $\alpha = MB/k_BT$, and k_B is Boltzmann's constant.

Like most other free-swimming bacteria, magnetotactic bacteria propel themselves through the water by rotating their helical flagella. The migration velocity v_m of the bacterium along **B** is given by the component of the forward swimming velocity v_0 along the direction of the field, $v_m = v_0 L(\alpha)$. For magnetotactic bacteria, migration velocities can be >80% of their forward velocities and are significantly faster than other motile bacteria that only have chemotactic or aerotactic responses to migrate up concentration gradients [5].

When cultured magnetotactic bacteria were studied in oxygen concentration gradients using thin, flattened capillaries, it became clear that magnetotaxis and aerotaxis work together in these bacteria [29]. The behavior observed in these strains has been referred to as "magneto-aerotaxis", and two different magneto-aerotactic mechanisms, termed polar and axial, are found in different bacterial species. For both polar and axial magnetotactic bacteria, the cellular magnetic dipole remains oriented along the local magnetic field, but the direction of migration along the magnetic field lines is determined by the sense of flagellar rotation, which in turn is controlled by aerotactic receptors. Thus a magnetotactic bacterium is essentially a self-propelled magnetic dipole with a "nose" (oxygen sensor). This is advantageous because aquatic habits have horizontal chemical stratification and moving up and down inclined geomagnetic field lines efficiently allows the cells to reach the optimal oxygen concentration [30]. Thus magnetotaxis effectively turns a three-dimensional search problem into a one-dimensional search problem along the magnetic field.

10. Conclusion

The magnetosome chain is a masterpiece of permanent magnet engineering that solves the problem of constructing a permanent magnetic compass needle that is sufficiently magnetic to be oriented in the geomagnetic field at ambient temperature, yet fits into a one-micron diameter cell and can be assembled *in situ*. The cells migrate along inclined magnetic field lines and use aerotaxis to efficiently locate and remain at the optimal oxygen concentration in the vertical oxygen concentration gradient in the water column or sediment.

While a single magnetosome chain would appear to be ideal, a number of magnetotactic bacteria have magnetosomes or magnetosome arrangements that depart from the ideal. The Brazilian bacteria with the large magnetosomes is one example. Not only are the magnetosomes MSD, but the cells have enough magnetosomes so that the calculated magnetic dipole moment of the cell is ca. 250 times larger than that of a typical cell of *M. magnetotacticum*. It is difficult to rationalize such a

big moment only on the basis of magnetic orientation in the geomagnetic field. There are also examples of magnetotactic bacteria that contain hundreds of SD magnetosomes [11, 31], also many more than required for orientation. One large, rod-shaped organism, *Magnetobacterium bavaricum*, contains up to 1000 bullet-shaped magnetosomes arranged in several chains traversing the cell [32]. Some bacteria have SD magnetosomes that are not arranged in chains, but are clustered on one side of the cell. In most of these cases, the magnetosomes have elongated habits and there is a consensus alignment of the elongation axes. In such an arrangement, the shape anisotropy of each crystal provides the stability against remagnetization, rather than the overall shape anisotropy in the magnetosome chain arrangement. These "non-ideal" arrangements may be pointing to additional functions of magnetosomes, possibly related to metabolism, that remain to be elucidated.

Acknowledgements

I thank Hendrik de Waard for his scientific insight and collaboration, and both Hendrik and Paula de Waard for their friendship and generosity of spirit.

References

1. de Waard, H., Hilsinger, J. and Frankel, R. B., *Rev. Sci. Instrum.* **72** (2001), 2724.
2. Penninga, I., de Waard, H., Moskowitz, B. M., Bazylinski, D. A. and Frankel, R. B., *J. Magn. Magn. Mater.* **149** (1995), 279.
3. Blakemore, R. P., *Annu. Rev. Microbiol.* **36** (1982), 217.
4. Bazylinski, D. A., Frankel, R. B., Heywood, B. R., Mann, S., King, J. W., Donaghay, P. L. and Hanson, A. K., *Appl. Environ. Microbiol.* **61** (1995), 3232.
5. Frankel, R. B., *Annu. Rev. Biophys. Bioeng.* **13** (1984), 85.
6. Balkwill, D. L., Maratea, D. and Blakemore, R. P., *J. Bacteriol.* **141** (1980), 1399.
7. Gorby, Y. A., Beveridge, T. A. and Blakemore, R. P., *J. Bacteriol.* **170** (1988), 834.
8. Baeuerlein, E. (ed.), *Biomineralization: From Biology to Biotechnology and Medical Application*, Wiley-VCH, Weinheim, 2000.
9. Ofer, S., Nowik, I., Bauminger, E. R., Papaefthymiou, G. C., Frankel, R. B. and Blakemore, R. P., *Biophys. J.* **46** (1984), 57.
10. Bazylinski, D. A. and Frankel, R. B., In: E. Baeuerlein (ed.), *Biomineralization: From Biology to Biotechnology and Medical Application*, Wiley-VCH, Weinheim, 2000, p. 25.
11. Vali, H. and Kirschvink, J. L., In: R. B. Frankel and R. P. Blakemore (eds.), *Iron Biominerals*, Plenum, New York, 1990.
12. Heywood, B. R., Mann, S. and Frankel, R. B., In: M. Alpert, P. Calvert, R. B. Frankel, P. Rieke and D. Tirrell (eds.), *Materials Synthesis Based on Biological Processes*, Materials Research Society, Pittsburgh, 1991.
13. Bazylinski, D. A., Garratt-Reed, A. J. and Frankel, R. B., *Microsc. Res. Tech.* **27** (1994), 389.
14. Devouard, B., Pósfai, M., Hua, X., Bazylinski, D. A., Frankel, R. B. and Buseck, P. R., *Am. Mineral.* **83** (1998), 1387.
15. Taylor, A. P., Barry, J. C. and Webb, R. I., *J. Micro.* **201** (2001), 84.
16. Dunlop, D. J. and Özdemir, Ö., *Rock Magnetism: Fundamentals and Frontiers*, Cambridge University Press, Cambridge, 1997.

17. Mann, S. and Frankel, R. B., In: Mann, J. Webb and R. J. P. Williams (eds.), *Biomineralization: Chemical and Biochemical Perspectives*, VCH, New York, 1989.
18. Banerjee, S. K. and Moskowitz, B. M., In: J. L. Kirschvink, D. S. Jones and B. J. MacFadden (eds.), *Magnetite Biomineralization and Magnetoreception in Organisms*, Plenum, New York, 1985.
19. Moskowitz, B. M., *Rev. Geophys. Supp.* (1995), 123.
20. Walker, M., Mayo, P. I., O'Grady, K., Charles, S. W. and Chantrell, R. W., *J. Phys. Condens. Matter.* **5** (1993), 2779.
21. Wittborn, J., Rao, K. V., Proksch, R., Revenko, I., Dahlberg, E. D. and Bazylinski, D. A., *Nanostructured Materials* **12** (1999), 1149.
22. Carter-Stiglitz, B., Moskowitz, B. M. and Jackson, M., *J. Geophys. Res.* **106** (2001), 26,297.
23. Lins, U., Solórzano, G. and Farina, M., *Bull. Instit. Océanograph Monaco* **14**(1) (1994), 95.
24. Farina, M., Kachar, B., Lins, U., Broderick, R. and Lins de Barros, H., *J. Microsc.* **173** (1994), 1.
25. Fabian, K., Kirchner, A., Williams, W., Heider, F., Leibl, T., Huber, A., *Geophys. J. Int'l.* **124** (1996), 89.
26. Dunin-Borkowski, R. E., McCartney, M. R., Frankel, R. B., Bazylinski, D. A., Posfai, M. and Buseck, P. R., *Science* **282** (1998), 2868.
27. Dunin-Borkowski, R. E., McCartney, M. R., Posfai, M., Frankel, R. B., Bazylinski, D. A. and Buseck, P. R., *Eur. J. Mineral.* **13** (2001), 671.
28. McCartney, M. R., Lins, U., Farina, M., Buseck, P. R. and Frankel, R. B., *Eur. J. Mineral.* **13** (2001), 685.
29. Frankel, R. B., Bazylinski, D. A., Johnson, M. and Taylor, B. L., *Biophys. J.* **73** (1997), 994.
30. Frankel, R. B. and Bazylinski, D. A., *Hyp. Interact.* **90** (1994), 135.
31. Thornhill, R. H., Burgess, J. G., Sakaguchi, T. and Matsunaga, T., *FEMS Microbiol. Lett.* **115** (1994), 169.
32. Spring, S., Amann, R., Ludwig, W., Schleifer, K.-H., van Germerden, H. and Petersen, N., *Appl. Environ. Microbiol.* **59** (1993), 2397.